

Energy Metabolism in Uncoupling Protein 3 Gene Knockout Mice*

Received for publication, December 22, 1999, and in revised form, March 15, 2000
Published, JBC Papers in Press, March 22, 2000, DOI 10.1074/jbc.M910179199

Antonio J. Vidal-Puig^{‡§}, Danica Grujic[‡], Chen-Yu Zhang[‡], Thilo Hagen[‡], Olivier Boss[‡],
Yasuo Ido[¶], Alicja Szczepanik[‡], Jennifer Wade[‡], Vamsi Mootha[‡], Ronald Cortright^{||},
Deborah M. Muoio^{||}, and Bradford B. Lowell^{‡**}

From the [‡]Division of Endocrinology, Department of Medicine, Beth Israel Deaconess Medical Center and Harvard Medical School, Boston, Massachusetts 02215, [¶]Departments of Exercise and Sports Science Physiology and Biochemistry, School of Medicine, East Carolina University, Greenville, North Carolina 27858, and [¶]Diabetes and Metabolism Unit, Boston Medical Center, Boston, Massachusetts 02118

Uncoupling protein 3 (UCP3) is a member of the mitochondrial anion carrier superfamily. Based upon its high homology with UCP1 and its restricted tissue distribution to skeletal muscle and brown adipose tissue, UCP3 has been suggested to play important roles in regulating energy expenditure, body weight, and thermoregulation. Other postulated roles for UCP3 include regulation of fatty acid metabolism, adaptive responses to acute exercise and starvation, and prevention of reactive oxygen species (ROS) formation. To address these questions, we have generated mice lacking UCP3 (UCP3 knockout (KO) mice). Here, we provide evidence that skeletal muscle mitochondria lacking UCP3 are more coupled (i.e. increased state 3/state 4 ratio), indicating that UCP3 has uncoupling activity. In addition, production of ROS is increased in mitochondria lacking UCP3. This study demonstrates that UCP3 has uncoupling activity and that its absence may lead to increased production of ROS. Despite these effects on mitochondrial function, UCP3 does not seem to be required for body weight regulation, exercise tolerance, fatty acid oxidation, or cold-induced thermogenesis. The absence of such phenotypes in UCP3 KO mice could not be attributed to up-regulation of other UCP mRNAs. However, alternative compensatory mechanisms cannot be excluded. The consequence of increased mitochondrial coupling in UCP3 KO mice on metabolism and the possible role of yet unidentified compensatory mechanisms, remains to be determined.

Uncoupling protein 3 (UCP3)¹ (1–3) is a member of the

* This work was supported by National Institutes of Health Grant DK49569 (to B. B. L.), a grant from Lilly (to B. B. L.), Boston Obesity Nutrition Research Center (BONRC) Pilot Project Award P30 DK46200 (to A. V.-P.), BONRC Transgenic Core Grant P30 DK46200, and Human Frontier Science Program Grant LT 0020/1999 (to O. B.). The costs of publication of this article were defrayed in part by the payment of page charges. This article must therefore be hereby marked "advertisement" in accordance with 18 U.S.C. Section 1734 solely to indicate this fact.

[§] Present address: University of Cambridge, Depts. of Clinical Biochemistry and Medicine, Addenbrooke's Hospital, Box 232, Cambridge CB2 2QR, UK.

** To whom correspondence should be addressed: Beth Israel Deaconess Medical Center, Endocrine Division, Research North Rm., 99 Brookline Ave., Boston, MA 02215. Tel.: 617-667-5954; Fax: 617-667-2927; E-mail: blowell@caregroup.harvard.edu.

¹ The abbreviations used are: UCP3, uncoupling protein 3; ROS, reactive oxygen species; PCR, polymerase chain reaction; RER, respiratory exchange ratio; WT, wild type; LDCL, lucigenin-derived chemiluminescence; FCCP, carbonyl cyanide *p*-(trifluoromethoxy) phenylhydrazone; KO mice, knockout mice; bp, base pair(s); HFD, high fat diet.

mitochondrial anion carrier superfamily with high homology (57%) to UCP1, a well characterized uncoupling protein (4, 5). UCP3 together with UCP1, UCP2 (6, 7), and possibly BMCP1 (brain mitochondrial carrier protein) (8) and UCP4 (9), form a family of uncoupling proteins located in the inner mitochondrial membrane. The evidence supporting the uncoupling activity of these proteins comes from studies where UCPs have been heterologously expressed in yeast or reconstituted into proteoliposomes. The expression of UCP2 and -3 decreases the mitochondrial membrane potential, as assessed by uptake of fluorescent membrane potential-sensitive dyes in whole yeast. They also increase state 4 respiration in isolated mitochondria, which serves as an indicator of inner membrane proton leak (3, 6, 10). More recently, reconstitution of UCPs into liposomes has shown that UCP2 and UCP3, like UCP1, mediate proton transport across bilipid layers (11).

It is well established that UCP1 is exclusively expressed in brown fat, where it plays a key role in facultative thermogenesis in rodents. Although there is controversy about the molecular mechanisms involved (12–16), it is clear that activated UCP1 catalyzes a proton leak across the mitochondrial inner membrane leading to thermogenesis. The activity of UCP1 is highly regulated, facilitated by fatty acids and inhibited by purine ribose di- and trinucleotides (ATP, ADP, GTP, GDP) (17). UCP1 is also highly regulated at the transcriptional level (18) by catecholamines, thyroid hormone, retinoids, and thiazolidinediones.

The characterization of the new uncoupling proteins (UCP2, UCP3, BMCP1, and UCP4) is in its early phases. UCP2 and UCP3 are of particular interest because they share the highest homology with UCP1 (57%) and are expressed in tissues that may be important for energy expenditure (see below). The tissue distribution of UCP1, UCP2, and UCP3 is markedly different. UCP2 is widely distributed (6, 7), whereas UCP3 expression is restricted to skeletal muscle and brown fat (1–3). It is well established that brown adipose tissue is an important tissue for thermogenesis in rodents. However, in large mammals in which brown fat is less common, skeletal muscle may be more important for thermogenesis (19). Thus, based upon the high homology with UCP1 and its expression in skeletal muscle, UCP3 has been suggested to play an important role in regulating energy expenditure, thereby influencing body weight regulation (1–3, 20).

UCP3, like UCP1, is highly regulated at the transcriptional level. Factors such as fatty acids (21–23), diet (24), exercise (25, 26), and fasting (27) markedly induce UCP3 expression in skeletal muscle. The induction of UCP3 during starvation, at a time when energy expenditure is decreased (28), does not support a primary role for UCP3 in energy dissipation. However,

data showing increases in circulating fatty acid levels associated with starvation, together with several findings linking UCP3 mRNA levels to fatty acid metabolism, suggest that UCP3 could be required for fatty acid metabolism. Thus, it is conceivable that UCP3 could facilitate the oxidation of fatty acids (29).

As is true for UCP1, it is likely that UCP3 activity is modulated by allosteric regulators. Based upon studies employing reconstituted proteoliposomes, it has been suggested that fatty acids are required for the uncoupling activity of UCP2 and UCP3 (11) and that UCP2 and UCP3 activities are inhibited by purine nucleotides. However, in contrast to UCP1, much higher concentrations of purine nucleotides are required for inhibition, and the maximal degree of inhibition is significantly less (11).

Other strategies have been used to clarify the function of UCP3 in humans. Using a genetic approach, linkage analysis studies suggest that UCP2 and UCP3 may influence resting metabolic rate (30). However, association studies indicate that variants of UCP2/3 are unlikely to contribute to the development of obesity (31). Of note, association studies in African-Americans report the existence of a mutation of the splice donor junction at exon 6 that results in exclusive production of UCP3S (29, 32) a truncated version of UCP3 lacking the last 37 C-terminal residues. Argyropoulos *et al.* (29) find that individuals heterozygous for this mutation showed reduced fatty acid oxidation and increased respiratory quotients (29). In contrast, a recent study including individuals homozygous for this mutation have not found abnormalities in the respiratory quotient (32).

It has also been proposed that UCP3 could prevent the formation of oxygen-free radicals in skeletal muscle. This hypothesis is based upon the observation that mitochondrial membrane potential regulates the production of reactive oxygen species (ROS) (33–37). According to this hypothesis, mild mitochondrial uncoupling could markedly decrease superoxide production by decreasing the mitochondrial membrane potential below a critical level. Thus, one of the functions of UCP3 could be to prevent the transmembrane electrochemical gradient from rising above a threshold critical for ROS formation (33, 35).

In summary, the information available about the physiological role of UCP3 is still controversial and incomplete. In the present study, we attempt to address these questions by using homologous recombination to create gene knockout mice lacking UCP3.

EXPERIMENTAL PROCEDURES

Targeting Construct and Embryonic Stem Cell Culture (Fig. 1)

Two UCP3 genomic clones were obtained after PCR screening of a P1 C129/SvJ genomic library (Genome System). Both clones were mapped using Southern blot analysis and end-labeled oligonucleotide probes designed according to mouse UCP3 cDNA sequence (GenBank™ accession number AF053352). A replacement targeting vector was prepared in which a segment of the UCP3 gene between exons 2 and 3, including the start codon, was removed and replaced with a PGK-NEO-poly(A) expression cassette (38). The targeting plasmid was linearized with *NotI* and electroporated into J1 embryonic stem cells provided by E. Li, A. Sharp, and R. Jaenisch (39). Selection with G418 was done as described (38). Drug-resistant clones were isolated and expanded followed by genomic DNA extraction for Southern blot analysis (Fig. 1). Three targeted clones were injected into C57B1/6 embryos at the blastocyst stage. Chimeric offspring were mated with C57B1/6 mice. Germ-line transmission of the mutant allele was determined by Southern analysis of mouse tail genomic DNA. Three lines of mice carrying the disrupted UCP3 were generated.

PCR Analysis

Genotyping was performed by multiplex PCR. Specific primers used to detect the KO allele were sense 5'-CCT CCA CTC ATG ATC TAT

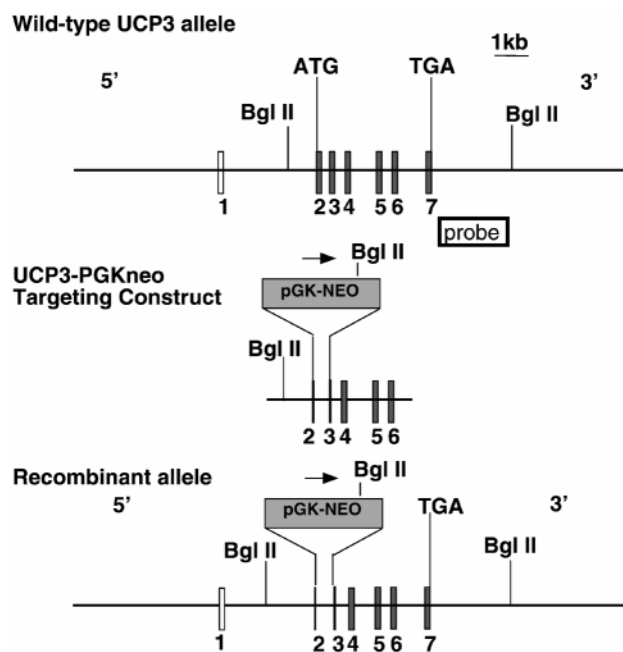


FIG. 1. The mouse UCP3 gene, targeting vector, and Southern blot detection scheme. Shown is a partial restriction enzyme map of the mouse UCP3 gene, the UCP3 KO targeting construct, and the predicted structure of the recombinant allele. The empirically determined map is consistent with a previously reported genomic map (24). The targeting construct contains approximately 8 kilobases (*kb*) of homologous mouse UCP3 genomic DNA, with 4 kilobases located 5' and 4 kilobases located 3' of the PGK-NEO-poly(A) cassette (61). The PGK-NEO-poly(A) cassette replaces approximately 700 bp of mouse UCP3 genomic sequence between restriction sites *SmaI* (exon 2) and *SacII* (exon 3). The Southern blot probe is located outside the targeting construct sequence. To detect targeted clones, genomic DNA was digested with *BglIII*. Filled boxes refer to exons corresponding to coding sequence, the locations of which have previously been published (24). The arrow refers to the orientation of transcription of the PGK-NEO cassette.

AGA TC-3', located in the neo cassette, and antisense 5'-ACC CTC TGT CGC CAC CAT AGT CA-3', located in the UCP3 coding sequence. This set of primers amplified a 300-bp PCR product. Primers used to detect the wild type allele were sense 5'-GCA CTG CGG CCT GTT TTG-3' and antisense 5'-ACC CTC TGT CGC CAC CAT AGT CA-3'. This set of primers amplified a 600-bp PCR product. Standard protocols were used for PCR.

Animal Care

Animals were housed four per cage in a temperature-controlled room with a 12-h light/dark cycle. Food and water were available *ad libitum* unless noted. All experiments were conducted in accordance with the National Institutes of Health (NIH) Guide for the Care and Use of Laboratory Animals.

Northern, Ribonuclease Protection, and Western Blot Analysis

Nucleic Acids—Isolation of nucleic acids (RNA, DNA) and Southern, Northern, and Ribonuclease protection assays were carried out as described previously (40, 41). Most of the probes were PCR-amplified using specific primers listed in Table I. A full-length rat UCP1 cDNA including the whole coding sequence was used as a probe. Isotopic bands were visualized by autoradiography and quantitated by PhosphorImager analysis using ImageQuant software (Molecular Dynamics, Sunnvale, CA).

Antibodies—Rabbit polyclonal antibody against mouse cytochrome *c* was purchased from Santa Cruz Biotechnology, Santa Cruz, CA (SC-7159). Mouse UCP3 antibody was obtained after rabbit immunization against a peptide (MIRLGTGGERKYRGTMDAYRC), corresponding to mouse and rat UCP3 amino acids 147–166 encoded by exon 4 (Covance Research Products, Denver, PA). Antisera was affinity-purified on a peptide column generated from the respective peptide coupled to a Sulfo-Link column (Pierce). UCP3 antibody was eluted with 0.1 M glycine, pH 2.5, and neutralized with 1 M Tris, pH 10.

SDS-Polyacrylamide Gel Electrophoresis Analysis and Immunoblotting—Western blot analyses were performed on isolated skeletal muscle

TABLE I
List of primers for Northern and RNase protection assay probes

mUCP3 (10–300 bp)
5'-GCT GCT ACC TAA TGG AGT GG-3'
5'-GTT CTC CCC TTG GAT CTG CAG-3'
mUCP3 (581–775 bp)
5'-AGG TCC GAT TTC AAG CCA TG-3'
5'-CAG GTG AGA CTC CAG CAA-3'
mUCP3 (740–1054 bp)
5'-GAT GGT GAC CTA CGA CAT CAT CAA GGA-3'
5'-AGG CCC TCT TCA GTT GCT CAT A-3'
mUCP3 (1015–1190 bp)
5'-CAT ATG AGC AAC TGA AGA GG-3'
3'-CGT GTC AGC AGC AGT GCA GGG-3'
mUCP2 (709–904 bp)
5'-CTG GTC GCC GGC CTG CAG CGC-3'
5'-GGG CAC CTG TGG TGC TAC CTG-3'

mitochondria (isolation of mitochondria describe below). Western blot analysis was performed as described previously (41).

Mitochondrial Oxygen Consumption

Mitochondria Isolation—Mitochondria were isolated from skeletal muscle of wild type ($n = 15$) and UCP3 KO mice ($n = 15$). Tissue was ground and homogenized in 10–20 ml of cold buffer (250 mM sucrose, 10 mM Hepes, 0.5 mM EDTA, pH 7.2 with KOH, 0.1% bovine serum albumin) and kept on ice. Homogenate was centrifuged at $600 \times g$ for 5 min. The pellet was discarded, and the supernatant was centrifuged at $8000 \times g$ for 10 min. The mitochondrial pellet was washed twice and finally resuspended in buffer without bovine serum albumin. The mitochondria were then used for immunoblotting, polarography, and assays of aconitase activity.

Polarography—Mitochondrial respiration was measured in a Clark-type oxygen electrode at 37 °C using the following incubation conditions: 250 mM sucrose, 10 mM Hepes, pH 7.2, 5 mM $\text{KH}_2\text{PO}_4/\text{K}_2\text{HPO}_4$, 0.5 mM EDTA, 5 mM malate, 10 mM glutamate, and approximately 0.5 mg of mitochondrial protein/ml. The data were channeled into an A/D converter and recorded on a Pentium-based PC using the DataShuttle A/D converter and the Quicklog software package. The oxygen electrode was calibrated with experimental buffer saturated with room air assuming a solubility coefficient of 199 nmol O_2/ml at 30 °C.

Determination of ATP, ADP, and Phosphocreatine Concentrations in Skeletal Muscle

Perchloric acid extracts of frozen muscle were prepared as follows. 100–200 mg of skeletal muscle (gastrocnemius) tissue were homogenized using a Polytron in 1.0 ml of 6% perchloric acid on ice. The samples were centrifuged for 1 min at $8000 \times g$. 600 μl of the supernatant were removed and neutralized by adding 300 μl of 0.4 M triethanolamine HCl, 1.6 M K_2CO_3 . ADP, ATP, and phosphocreatine were measured enzymatically as described previously by Jaworek *et al.* (42).

Oxygen Consumption (VO_2) and Respiratory Exchange Ratio (RER)

Oxygen consumption and respiratory exchange ratio were measured in 10-week-old UCP3 knockout and wild type mice in basal and fasted conditions (5 mice per group and treatment) using the OXYMAX System 4.93 (Columbus Instruments, Columbus, OH) and conditions of a settling time of 100 s, measuring time of 50 s, and room air as a reference. Animals were placed individually in 4 0.3-liter chambers. Results are expressed as ml/kg/min. To correct for body size, results are also expressed as ml/kg^{2/3}/min.

Influence of UCP3 on Body Weight, Food Intake, and Thermogenesis

Body Weight—UCP3 KO and wild type mice body weights were recorded weekly for 18–22 weeks ($n = 9$ –12 per group and treatment). The effect of chow diet (Richmond Stenolard #5008) and a high fat diet (Research Diets Inc #D12451) on the evolution of body weight was assessed. Chow diet = 10% fat, 70% carbohydrate, and 20% protein (as percent of total calories); high fat diet = 45% fat, 35% carbohydrate, and 20% protein (as % of total calories). Both genders and the three possible genotypes (+/+, +/-, -/-) were studied.

Muscle Weights—Tibialis anterior, soleus, and heart were carefully dissected and weighed. To correct for differences in muscle weight due to differences in age and body weight, results are expressed as absolute weight and as the ratio muscle weight (g)/total body weight.

Carcass Analysis Was Performed in Male Animals—Specifically, we studied wild type mice on chow ($n = 9$) and high fat diets ($n = 8$) and UCP3 KO mice on chow ($n = 11$) and high fat diets ($n = 9$). Total body lipid content was assessed using alcoholic potassium hydroxide digestion with saponification of all fats, neutralization, and then enzymatic determination of glycerol as described previously (44). Triglyceride content is expressed as g/carcass and as percentage of total body weight.

Food Intake—Food intake was measured in 10-week-old UCP3 KO female ($n = 7$), UCP3 KO male ($n = 5$), control female ($n = 8$), and control male ($n = 8$) mice for 3 weeks after a 1-week period of adaptation. Animals were housed individually and had free access to water. Food was weighed weekly, and the differences were assumed to represent grams of food eaten per week. Data are presented as g/day. To correct for body size, results are also expressed as g/day/body weight^{2/3}. The cages were inspected for food spillage, and none was noted.

Thermogenesis—Rectal temperature was assessed using a rectal probe (Yellow Spring Instruments Co.) in control (C) and UCP3 KO mice under the following situations: (a) fed state (C, $n = 9$; KO, $n = 9$) and (b) following 1, 4, and 24 h of cold exposure (C, $n = 5$; KO, $n = 5$).

Effects of Exhaustive Exercise

Animals—Thirty-two mice (5–9 months old) were matched for age and randomly divided into four groups as follows: 1) wild type-sedentary; 2) wild type-exercised; 3) UCP3 KO-sedentary; 4) UCP3 KO-exercised. Animals were given water and fed *ad libitum* and were maintained on a 12-h light/dark cycle.

Exercise Protocol—On the day before the exercise test, mice (wild type (WT) = 9, KO = 9) were accommodated to the treadmill apparatus and run twice for 2 h with a 30-min rest period between each running protocol. Within each 2-h running trial, the mice ran to physical exhaustion according to the following protocol: mice were accommodated to the treadmill apparatus by running at 10 meters/min for 10 min at 0% grade. Afterward, the treadmill speed was increased by 5 meters/min every 30 min so that the animals were running at a final speed of 30 meters/min for the final half of the 2-h protocol. The percentage grade of the treadmill was increased at 60 (3%), 90 (6%), and 105 min (9%). The animals continued to run at 30 meters/min up the 9% grade until they became physically exhausted (inability to avoid a shock device located in the back of the running stall) or the test was terminated at 2 h. The time (seconds) to exhaustion was recorded, and exhaustion was verified by the absence of a righting reflex (inability of the animal to right itself when placed on its back). Because UCP3 activity might be bioenergetically necessary to recover from vigorous exercise challenge, the mice rested for 30 min, and the protocol was repeated to evaluate their exercise capacity following recovery. The following day, the same 2 h running protocol to exhaustion was employed, and assessment of skeletal muscle carbohydrate and lipid metabolism was made immediately post-exercise.

Muscle Glucose and Fatty Acid Oxidation

Food was withdrawn from both sedentary and exercised animals 3 h before the exercise test. Immediately after exercise, animals were anesthetized (ketamine/xylazine, 100 mg/10 mg/kg), and soleus and extensor digitorum longus muscles were excised, cleaned of adipose and connective tissue, and transferred to a 24-well tissue culture plate in a shaking bath at 29 °C. One soleus and one extensor digitorum longus were used to measure fatty acid oxidation, and contralateral muscles were used to determine glucose oxidation. Muscles were incubated as described previously (45) in 1.0 ml of modified Krebs-Henseleit buffer continuously gassed with 95% O_2 , 5% CO_2 . After 15 min at 29 °C, muscles were placed in fresh modified Krebs-Henseleit buffer containing 1.0 mmol/liter sodium oleate, 1.0 mmol/liter carnitine, and 1% bovine serum albumin and pre-incubated for an additional 20 min at 37 °C. Muscles were then transferred to identical media but with either [^{14}C]glucose (1.0 mCi/ml) or [^{14}C]oleate (1.0 mCi/ml) and incubated 90 min at 37 °C. Afterward, the CO_2 produced by muscle was driven from the media by adding 100 μl of 70% perchloric acid to each well. [^{14}C] CO_2 was trapped onto NaOH-saturated Whatman No. 3 filter paper, and oxidation rates were quantified as described previously (45).

Blood Glucose and Insulin Determinations

Blood glucose and insulin determinations were obtained after an overnight fast and in fed animals (obtained between 8 a.m. and noon) using a glucometer (One Touch, Lifescan, Milpitas, CA) and an enzyme-linked immunosorbent assay (Crystal Chem Inc. Chicago, IL) with rat insulin as a standard. Free fatty acids were measured using a commercially available kit (Wako NEFA C kit, Wako Chemicals, Richmond,

VA). Triglycerides (#337), β -hydroxybutyrate (#310-UV), creatine phosphokinase (#520), lactate (#735-10), and blood urea nitrogen (#535) were measured using kits from Sigma.

Oxygen Free Radical Studies in Skeletal Muscle Mitochondria

Measurement of Mitochondrial Superoxide Anion Production by Lucigenin-derived Chemiluminescence (LDCL) (46)—LDCL was measured at 25 °C using a Berthold luminometer. The incubation conditions were as follows: 70 mM sucrose, 220 mM mannitol, 2 mM Hepes, pH 7.4, 2.5 mM potassium phosphate, 0.5 mM EDTA, 5 mM malate, 10 mM glutamate, 20 μ M lucigenin. After recording the background LDCL for 4 min, the assay was initiated by the addition of 0.1 mg/ml mitochondria. LDCL was recorded for 10 min in 2-min intervals, and the data were expressed as the integrated area under the curve. The effects of a superoxide dismutase mimetic (47) (SC52608, Monsanto Corporate Research, St. Louis, MO) and an uncoupler, 1 μ M carbonyl cyanide *p*-(trifluoromethoxy) phenylhydrazone (FCCP), on lucigenin chemiluminescence were assessed as controls.

Mitochondrial Aconitase Activity in Isolated Mitochondria Was Measured Following the Protocol of Hausladen and Fridovich (48)—Mitochondria were isolated, 40–60 μ g of mitochondria were incubated in 1% Triton X-100, and the extract was resuspended in buffer containing 50 mM Tris-Cl pH 7.4, 30 mM sodium citrate, 0.6 mM MnCl₂, 0.2 mM NADP, 1–2 units of isocitrate dehydrogenase (Sigma I-2516, derived from porcine heart). After adding the mitochondrial extract, the absorbance at 340 nm increased at a rate corresponding to aconitase activity. The level of aconitase activity measured in the mitochondrial extract equals active aconitase (basal level). Aconitase inhibited by ROS *in vivo* was reactivated so that total activity could be measured by incubating mitochondrial extracts with 0.5 M dithiothreitol, 20 mM Na₂S, and 20 mM ferrous ammonium sulfate. Aconitase activity, measured after reactivation, equals the total aconitase activity. Results are expressed as the basal/total aconitase activity ratio (48).

Statistical Analysis

Statistical analysis was performed using StatView 4.0 (Abacus Concept, Berkeley, CA). Results are presented as the mean \pm S.E. Unpaired Student's *t* test and analysis of variance were performed as specified in figure and table legends (a *p* value 0.05 was used for significance).

RESULTS

UCP3 KO Mice Lack UCP3 mRNA and Protein—We developed an RNase protection assay that allows quantitation of mRNAs encoding mouse UCP3. We confirmed that the mRNA sequence corresponding to exons 2–6 was absent in skeletal muscle (Fig. 2A) and brown adipose tissue of UCP3 KO mice (data not shown). Western blotting analysis using an antibody raised against a peptide corresponding to the sequence encoded by exon 4 of UCP3 identified a band of the expected size (34 kDa) in the WT skeletal muscle mitochondria (Fig. 2B). This band was absent in UCP3 KO skeletal muscle mitochondria.

UCP3 KO Mice Do Not Have Compensatory Up-regulation of UCP1, UCP2, and BMCP1—UCP1 and UCP2 mRNAs were quantified by Northern blot and RNase protection assay analysis, respectively, using total RNA isolated from interscapular brown adipose tissue and gastrocnemius muscle. UCP2 mRNA in skeletal muscle (WT 239 \pm 19 versus KO 258 \pm 12 arbitrary units), *n* = 6) (Fig. 2D) and UCP1 mRNA in brown adipose tissue (WT 265 \pm 24 versus KO 283 \pm 35 arbitrary units, *n* = 6) were not up-regulated in UCP3 KO mice. UCP2 was not up-regulated in UCP3 KO brown adipose tissue (WT 372 \pm 25 versus KO 349 \pm 31, *n* = 6; not shown), and UCP1 mRNA was not detected in skeletal muscle (data not shown). Expression of BMCP1 (8) mRNA in skeletal muscle was assessed but was barely detectable in control mice and was not up-regulated in UCP3 KO animals (results not shown).

Respiration in UCP3 KO Skeletal Muscle Mitochondria—Respiration was measured in isolated skeletal muscle mitochondria from control and UCP3 KO male mice. An average of 15 independent experiments with at least two repeats per experiment were performed. As is shown in Fig. 3, UCP3 KO mice had an increased state 3/state 4 ratio (*, *p* = 0.002), which was due to a decrease in

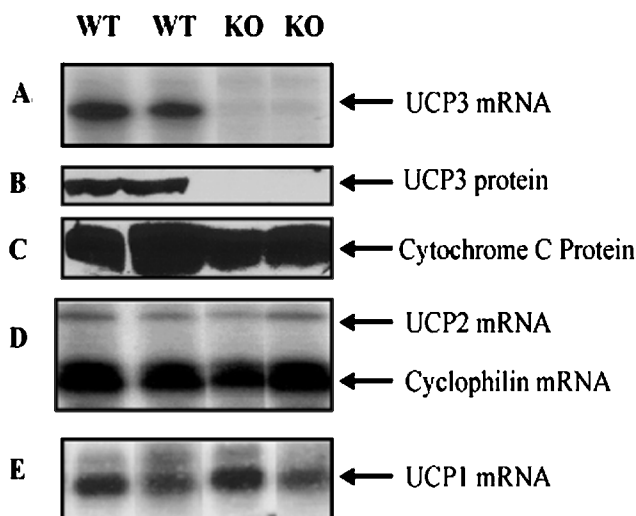


Fig. 2. Expression of UCP1, UCP2, and UCP3. A, UCP3 RNase protection assay. UCP3 and cyclophilin mRNA levels were determined using 10 μ g of skeletal muscle RNA as described under "Experimental Procedures." The UCP3 mouse probe corresponds to exons 6–7, and the expected protected band was 314 bp. Genotypes (WT and KO) were previously determined by PCR of tail genomic DNA. B, immunoblotting with UCP3 mouse polyclonal antibody. Samples correspond to proteins (50 μ g) derived from isolated skeletal muscle mitochondria of UCP3 KO and WT mice. Proteins were separated by SDS-polyacrylamide gel electrophoresis (12–15%) followed by western immunoblotting. UCP3 is a 34-kDa protein. C, immunoblotting with cytochrome *c* antibody (14 kDa) was used as an internal control. D, UCP2 RNase protection assay. UCP2 mRNA was measured using 10 μ g of total RNA isolated from gastrocnemius muscle of 8-week-old mice. Cyclophilin was used as an internal control. E, UCP1 mRNA Northern blot analysis. UCP1 mRNA levels were determined by Northern blot analysis using 20 μ g of total RNA isolated from interscapular brown adipose tissue. Northern blot and RNase protection assay protocols were performed and analyzed using a PhosphorImager as described under "Experimental Procedures."

state 4 respiration (*, *p* = 0.01). State 3 respiration was similar in WT and UCP3 KO mitochondria. These results indicate that a lack of UCP3 in skeletal muscle mitochondria increases the coupling of mitochondrial respiration to ADP availability, establishing for the first time that endogenous levels of UCP3 uncouple mammalian mitochondria.

Skeletal Muscle Weight, ATP, ADP, and Phosphocreatine Content—We investigated whether the lack of UCP3 resulted in any changes in skeletal muscle weights. As shown in Table II, the weights of several muscles (tibialis anterior, soleus, and heart) were similar in WT and UCP3 KO mice. Also, no statistically significant differences in the absolute values of ATP, ADP, or creatine phosphate were observed in skeletal muscle of UCP3 KO mice. However, ADP tended to be lower, and the ATP/ADP ratio tended to be higher in UCP3 KO mice (Table II).

Effect of UCP3 Deficiency on Body Weight Regulation, Total Body Triglyceride Content, and Food Intake—We studied whether the lack of UCP3 resulted in the development of obesity or predisposed to diet-induced obesity. Male and female UCP3 KO, UCP3 heterozygous, and wild type mice were weighed at 1-week intervals for 18–22 weeks (Fig. 4; data not shown for heterozygotes). The effects of two diets (chow and high fat diet) on body weight were studied. On the chow diet, no statistical differences in body weight were observed between groups. Male UCP3 KO mice fed a high fat diet tended to weigh more than wild type mice but the difference, probably due to body weight variability, did not reach statistical significance. Female mice of all genotypes fed a high fat diet were similar in body weight. Carcass analysis (g of triglyceride per carcass and percentage of fat per carcass) of chow and high fat fed male

FIG. 3. Mitochondrial oxygen consumption. O_2 consumption was measured in isolated skeletal muscle mitochondria from wild type and UCP3 KO male mice as described under "Experimental Procedures." Data represent an average of 15 independent experiments. Each separate experiment was repeated at least twice. Unpaired Student's *t* test: *, $p = 0.01$; **, $p = 0.002$ versus wild type.

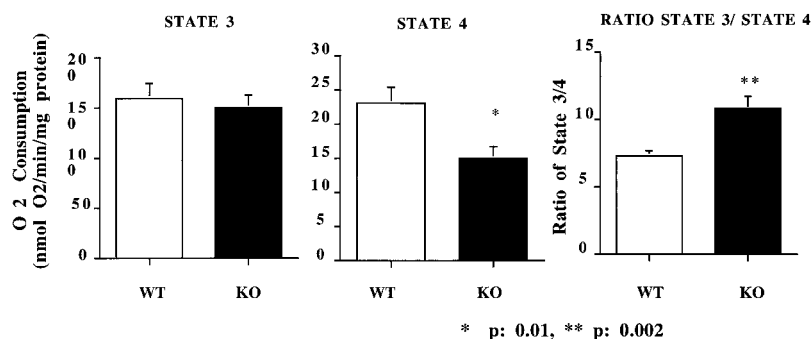


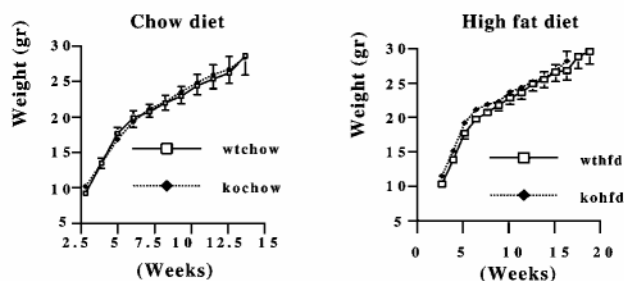
TABLE II
Measurements in skeletal muscle

Unpaired Student's *t* test was used for the statistical analysis. No significant differences were observed. Het, heterozygote; TA, tibiales anterior; SO, soleus. Results are expressed as absolute weight (abs) (mg, mean \pm S.E.) and corrected (abs \times 1000/total body weight).

Gender	Diet	Genotype	Weight of muscles		
			TA (abs/corrected)	SO (abs/corrected)	Heart (abs/corrected)
Male	Chow	WT	92 \pm 3/2.7 ($n = 11$)	19 \pm 1/0.54 ($n = 10$)	155 \pm 8/ 4.8 ($n = 8$)
Male	Chow	KO	93 \pm 3/2.6 ($n = 16$)	18 \pm 1/0.51 ($n = 16$)	161 \pm 10/4.9 ($n = 11$)
Male	HFD	WT	80 \pm 5/1.9 ($n = 9$)	19 \pm 1/0.46 ($n = 9$)	156 \pm 12/4.1 ($n = 4$)
Male	HFD	KO	98 \pm 3/1.9 ($n = 11$)	20 \pm 1/0.40 ($n = 11$)	184 \pm 10/3.6 ($n = 5$)

	ATP, ADP, and creatine phosphate in skeletal muscle	
	WT	KO
ATP (μ mol/g tissue)	5.13 \pm 0.39	5.10 \pm 0.59 $n = 5$
ADP (μ mol/g tissue)	0.94 \pm 0.15	0.67 \pm 0.15 $n = 5$
ATP/ADP	5.76 \pm 0.54	7.53 \pm 0.34 $n = 5$
Creatine phosphate (μ mol/g tissue)	8.80 \pm 0.30	8.70 \pm 0.60 $n = 5$

Females



Males

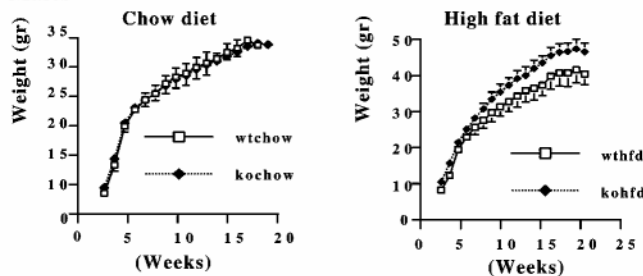


FIG. 4. Growth curves. Diet study. UCP3 KO (*kochow*) and wild type (*wtchow*) controls were weighed at 1-week intervals for 18–22 weeks. The effect of two diets (chow and high fat diet) was assessed. All three genotypes (+/+, +/-, -/-) were studied; however, only growth curves from WT and KO mice are shown. The number of animals used in this experiment was 9–12 animals per group. Data are the mean \pm S.E. Factorial and repeated analysis of variance were performed, and no statistically significant differences were detected.

mice revealed no statistically significant effect of genotype on total body lipid content (Table III). Total food intake was measured in a different set of 8-week-old mice that were fed a chow diet for 3 weeks. No differences in food intake (g/day) were

observed between UCP3 KO and control mice.

The Lack of UCP3 Does Not Modify the Respiratory Exchange Ratio (RER) and Rates of Oxygen Consumption (VO_2) (Table III)—Mice in the fed and fasted (24 h) state were studied. As expected, fasting was associated with a decrease in VO_2 (*, $p < 0.05$) due to a decrease in energy expenditure (49), and in RER ($p < 0.001$), due to preferential use of lipids as fuel. However, no differences were observed in O_2 consumption and RER between control and UCP3 KO mice, either in the fed or fasted state.

The Lack of UCP3 Does Not Affect Maintenance of Body Temperature during Cold Exposure (Table III)—In this study we addressed the potential role of UCP3 in thermoregulation. Rectal temperature was assessed in WT and UCP3 KO mice in the fed state ($n = 9$ per group). No statistical differences between WT and KO mice were observed. To study the thermogenic adaptation of UCP3 KO mice to cold environment, mice were housed at 4 °C, and their rectal temperatures were measured after 1, 4, and 24 h. No differences were observed between WT and KO mice at any time point.

Plasma Free Fatty Acids and Other Blood Parameters (Table IV)—As an initial approach to evaluate the potential role of UCP3 in fatty acid homeostasis, plasma free fatty acids levels were measured in three specific situations: (a) in newborn mice (4–6 days old) that depend exclusively on milk ingestion (rich in fatty acids); (b) in young (6 weeks old) mice in the fed (chow diet) and fasted state (36 h); and (c) in 18–24-week old mice in the fed (on chow and high fat diets) and fasted states (36 h after a chow diet). Free fatty acids tended to increase in the 18–24-week-old UCP3 KO mice. This difference was statistically significant in the 18–24-week-old group challenged with a high fat diet (Table IV). No statistical differences in plasma fatty acid levels were observed either in newborn mice or 6-week-old mice in the fed or fasted state. Other blood parameters such as triglycerides, β -hydroxybutyrate, creatine kinase, lactate, glu-

TABLE III
 Measurements in the whole animal

NS, not statistically significant between genotype (WT vs. KO); Tgl, triglycerides; bw, body weight. Unpaired Student's *t* test and analysis of variance *post hoc* test were used for statistical analysis.

	WT	KO	
Food intake (g/day)			
Males	4.6 ± 0.08 <i>n</i> = 7	4.7 ± 0.14 <i>n</i> = 5	NS
Females	4.1 ± 0.24 <i>n</i> = 8	4.0 ± 0.24 <i>n</i> = 8	NS
Food intake (g/day/bw ^{2/3})			
Males	0.58 ± 0.04 <i>n</i> = 7	0.55 ± 0.18 <i>n</i> = 5	NS
Females	0.52 ± 0.02 <i>n</i> = 8	0.53 ± 0.14 <i>n</i> = 8	NS
Carcass (g Tgl/carcass)			
Chow	7.2 ± 1.2 <i>n</i> = 9	6.9 ± 1.0 <i>n</i> = 11	NS
HFD	10.2 ± 0.9 <i>n</i> = 8	9.1 ± 1.5 <i>n</i> = 9	NS
Carcass (% fat)			
Chow	23.9 ± 4.1 <i>n</i> = 9	22.7 ± 3.4 <i>n</i> = 11	NS
HFD	26.8 ± 2.3 <i>n</i> = 8	20.1 ± 3.3 <i>n</i> = 9	NS
Temperature (° C)			
Basal	35.3 ± 0.3 <i>n</i> = 10	35.6 ± 0.3 <i>n</i> = 10	NS
1-h cold	33.5 ± 0.5 <i>n</i> = 5	32.8 ± 0.7 <i>n</i> = 5	NS
4-h cold	33.7 ± 0.3 <i>n</i> = 8	33.1 ± 0.4 <i>n</i> = 8	NS
24-h cold	34.6 ± 0.2 <i>n</i> = 4	34.4 ± 0.4 <i>n</i> = 4	NS
RER			
Fed	0.84 ± 0.01 <i>n</i> = 5	0.84 ± 0.01 <i>n</i> = 5	NS
Fast	0.75 ± 0.01 <i>n</i> = 5	0.73 ± 0.01 <i>n</i> = 5	NS
O ₂ consumption (VO ₂) (ml/kg/min)			
Fed	37.2 ± 3.0 <i>n</i> = 5	38.0 ± 2.4 <i>n</i> = 5	NS
Fast	30.0 ± 1.9 <i>n</i> = 5	32.0 ± 1.2 <i>n</i> = 5	NS
(ml/kg ^{2/3} /min)			
Fed	109.9 ± 8.2 <i>n</i> = 5	117.6 ± 7.3 <i>n</i> = 5	NS
Fast	84.1 ± 5.6 <i>n</i> = 5	94.3 ± 5.5 <i>n</i> = 5	NS

cose, and insulin were similar in WT and KO mice (Table IV).

Effects of Exhaustive Exercise on Physical Performance and on Skeletal Muscle Glucose and Fatty Acid Oxidation—Exercise is associated with a dramatic increase in skeletal muscle ATP utilization. To support increased ATP requirements, ATP synthesis must be stimulated accordingly. To address the role of UCP3 in this response, mice were challenged with a protocol of acute exercise. This protocol included a progressive increase in the speed and uphill gradient of the treadmill for 2 h or until mice were exhausted. To study the recovery capacity post-exercise, a similar protocol was repeated after 30 min of rest. Two animals from each group failed to complete the initial part of the test, whereas the remaining mice ran for the required 2 h. None of the conditions tested revealed any alteration in the physical performance of UCP3 KO mice. Similarly, no differences were observed in their recovery capacity post-exercise.

We investigated whether skeletal muscle carbohydrate and lipid metabolism were affected during rest and exhaustive exercise. To address this, fatty acid and glucose oxidation were measured in soleus and extensor digitorum longus muscles from sedentary and exercised mice. No differences in fatty acid or glucose oxidation were observed between WT and KO mice (Table V). With exercise, there was a trend for fatty acid oxidation to decrease and for glucose oxidation to increase in both WT and KO mice.

Reactive Oxygen Species Production by UCP3 KO Skeletal Muscle Mitochondria—We explored the possibility that the lack of UCP3 resulted in increased production of ROS. We first investigated whether skeletal muscle mitochondria lacking UCP3 produced more superoxide anions. Isolated skeletal muscle mitochondria from 6–8-week-old UCP3 KO and WT mice were used to measure LDCL in the absence of ADP using glutamate and malate as respiratory substrates. To confirm the specificity of the LDCL assay, we added a superoxide dismutase mimetic compound (SC52608), an uncoupler (FCCP), and ADP. SC52608 scavenged oxygen free radicals, whereas FCCP and ADP decreased mitochondrial membrane potential,

FCCP by its cycling protonophore activity and ADP by stimulating ATP synthase. The LDCL-integrated area was inhibited by 50% with ADP, by 87% with SC52608, and by 100% with FCCP (Fig. 5A). Finally, using a yeast heterologous system expressing UCP1, we found that inhibition of UCP1 uncoupling activity with GDP resulted in an increase of luciferin chemiluminescence (Fig. 5B).

The LDCL integrated area of isolated skeletal muscle mitochondria from UCP3 KO mice was 58 ± 10% higher compared with control mitochondria (Fig. 5A). These data suggest that superoxide anion production is increased in skeletal muscle mitochondria from UCP3 KO mice.

We then measured mitochondrial aconitase activity as an *in vivo* indicator of ROS production. Mitochondrial aconitase activity was reduced by 20% (*p* < 0.01) in isolated muscle mitochondria from 6–8-week-old UCP3 KO mice (Fig. 5C). No differences in aconitase activity were observed between mitochondria isolated from the liver of UCP3 KO and WT mice (data not shown). No differences in total aconitase activity after reactivation were observed, indicating that UCP3 KO and WT skeletal muscle mitochondria contained similar amounts of total aconitase. These observations indicate that UCP3 KO skeletal muscle mitochondria overproduce ROS *in vivo*.

DISCUSSION

Uncoupling protein 3 is a member of the mitochondrial anion carrier superfamily. Based upon its high homology with UCP1 and its restricted tissue distribution to skeletal muscle and brown adipose tissue, it has been suggested that this protein could play important roles in regulating energy expenditure, body weight homeostasis, and thermoregulation. Identification of various physiologic states in which UCP3 mRNA levels are increased have led to the proposal that UCP3 may play roles in fatty acid metabolism and adaptive responses to acute exercise and starvation. It has also been suggested that the uncoupling activity of this protein may prevent the production of oxygen reactive species in mitochondria (35). To address these issues,

TABLE IV
Blood determinations

All measurements performed in 8–10-week-old male mice except where noted. Analysis of variance *post hoc* test Bonferroni/Dunn was used for statistical analysis.

	WT	KO
Triglycerides (mM)		
Chow	0.59 ± 0.10 <i>n</i> = 8	0.69 ± 0.10 <i>n</i> = 11
HFD	1.02 ± 0.20 <i>n</i> = 5	0.90 ± 0.10 <i>n</i> = 5
Fast	0.62 ± 0.02 <i>n</i> = 7	0.60 ± 0.10 <i>n</i> = 7
β-Hydroxybutyrate (μmol/liter)		
Fed	260 ± 40 <i>n</i> = 8	270 ± 50 <i>n</i> = 8
Fast	1030 ± 150 <i>n</i> = 5	1270 ± 120 <i>n</i> = 5
Urea (mg/dl)		
Chow	13.1 ± 4.0 <i>n</i> = 5	13.9 ± 4.0 <i>n</i> = 5
HFD	9.8 ± 1.0 <i>n</i> = 5	10.5 ± 0.5 <i>n</i> = 5
Creatine kinase (μmol/min/liter)		
Fed	50 ± 10 <i>n</i> = 10	41 ± 9 <i>n</i> = 6
Fast	196 ± 34 <i>n</i> = 9	243 ± 35 <i>n</i> = 7
Lactate (μmol/liter)		
Fed	3814 ± 720 <i>n</i> = 9	3993 ± 377 <i>n</i> = 7
Fast	2176 ± 301 <i>n</i> = 5	1998 ± 257 <i>n</i> = 6
Glucose (mg/dl)		
Chow	144 ± 6 <i>n</i> = 20	154 ± 5 <i>n</i> = 20
Fast (post-chow)	77 ± 4 <i>n</i> = 9	78 ± 4 <i>n</i> = 10
HFD	218 ± 19 <i>n</i> = 5	195 ± 17 <i>n</i> = 5
Fast (post-HFD)	97 ± 11 <i>n</i> = 5	100 ± 18 <i>n</i> = 5
Insulin (pg/ml)		
6–8 weeks		
Chow	1319 ± 209 <i>n</i> = 11	795 ± 112 <i>n</i> = 7
Fast	445 ± 40 <i>n</i> = 6	617 ± 123 <i>n</i> = 7
HFD	2907 ± 89 <i>n</i> = 4	3107 ± 201 <i>n</i> = 4
18–22 weeks		
Chow	1334 ± 428 <i>n</i> = 5	2767 ± 678 <i>n</i> = 10
Fast	273 ± 84 <i>n</i> = 6	260 ± 89 <i>n</i> = 6
HFD	3325 ± 1057 <i>n</i> = 7	5117 ± 1139 <i>n</i> = 7
Fatty acids (mM)		
3–6 days	0.67 ± 0.04 <i>n</i> = 6	0.58 ± 0.05 <i>n</i> = 8
6–8 weeks		
Chow	0.46 ± 0.04 <i>n</i> = 10	0.55 ± 0.05 <i>n</i> = 10
Fast	0.95 ± 0.06 <i>n</i> = 9	0.74 ± 0.06 <i>n</i> = 11
18–22 weeks		
Chow	0.52 ± 0.16 <i>n</i> = 5	0.74 ± 0.16 <i>n</i> = 10
Fast	0.95 ± 0.06 <i>n</i> = 6	1.13 ± 0.12 <i>n</i> = 6
HFD	0.45 ± 0.06 <i>n</i> = 5	0.87 ± 0.08 <i>n</i> = 8 ^a

^a *p* < 0.05.

we have generated and characterized the phenotype of mice lacking UCP3.

UCP3 KO mice appear to be healthy animals. They do not have gross morphological alterations, and they do not develop obesity. Their resting energy expenditure and thermoregulation are normal, and they appear to be similar to wild type mice in their tolerance for exercise. However, our data provide clear biochemical evidence that respiration in skeletal muscle mitochondria lacking UCP3 is abnormal. Indeed, UCP3 KO skeletal muscle mitochondria are more coupled, as evidenced by an increased respiratory control ratio (state 3/state 4). This higher coupling is due to a fall in state 4 respiration, which represents respiration due to proton leak. This observation is important because it represents the first clear evidence that UCP3, expressed at physiological levels in muscle, has proton transport activity and consequently functions as a genuine uncoupling protein.

Our results show that the lack of UCP3 is not associated with obesity. No differences in body weight, triglyceride content, and food intake were observed. Only UCP3 KO male mice challenged with high fat diet tended to be heavier (however, this was not statistically significant). These data indicate that UCP3 is not required for normal body weight regulation. This observation may not be completely surprising, since the genetic disruption of another uncoupling protein, UCP1, did not result

TABLE V

Fatty acid and glucose oxidation in skeletal muscle

Unpaired Student's *t* test was used for statistical analysis. EDL, extensor digitorum longus.

	WT	KO
Rate of oleate oxidation in skeletal muscle (nmol/g/h)		
Soleus		
Sedentary	130 ± 26	127 ± 30 (<i>n</i> = 6)
Exercise	131 ± 17	132 ± 22 (<i>n</i> = 6)
EDL		
Sedentary	156 ± 23	146 ± 25 (<i>n</i> = 6)
Exercise	108 ± 24	112 ± 19 (<i>n</i> = 6)
Rate of glucose oxidation in skeletal muscle (nmol/g/h)		
Soleus		
Sedentary	419 ± 96	385 ± 75 (<i>n</i> = 6)
Exercise	418 ± 57	394 ± 39 (<i>n</i> = 6)
EDL		
Sedentary	566 ± 103	517 ± 117 (<i>n</i> = 5)
Exercise	651 ± 93	601 ± 73 (<i>n</i> = 5)

in obesity (50). Since UCP2 mRNA levels are elevated in brown fat of UCP1 KO mice, it has been suggested that UCP2 might account for the lack of obesity in these mice. Against this idea is the observation that up-regulation of UCP2 in UCP1 KO mice failed to compensate with respect to cold sensitivity (50). Mice lacking UCP3 are not obese, are not cold sensitive, and they do not have up-regulation of either UCP2 or UCP1 mRNAs. This suggests that UCP3 may not play an important role in regulating body weight or adaptive thermogenesis in response to cold exposure. However, it cannot be excluded that the lack of UCP3 activity could be compensated through post-translational activation of UCP2 and/or UCP1 activity or, alternatively, through activation of other unknown futile cycles. Thus, double and triple UCP knockout mice would be useful tools to address these questions.

Several earlier studies suggest that free fatty acids induce the expression of UCP3 *in vivo* (21, 51) and *in vitro* (22). These observations and others (23) suggest that UCP3 may have a role in fatty acid metabolism, possibly by facilitating the oxidation of fatty acids. However, no statistical differences in blood fatty acid levels were observed in newborn mice (4 to 6 days post-delivery) and young mice (6 weeks). However, the study of 18- to 24-week-old animals revealed that UCP3 KO mice tended to have higher fatty acid levels in blood reaching statistical significance when challenged with a high fat diet. These results raise the possibility of an age-related progressive deterioration of fatty acid homeostasis in UCP3 KO mice. However, the mechanism for such an effect is unknown.

The analysis of fatty acid and glucose oxidation at rest and post-exercise did not reveal any differences between WT and KO skeletal muscle. Although several gene expression studies (21, 23, 51) and a study in humans (29) point to a role of UCP3 in fatty acid oxidation, our studies in isolated muscles (free fatty acid oxidation) and in whole animals (RER) indicate that UCP3 is not required for normal rates of fatty acid oxidation in mice.

Although UCP3 KO skeletal muscle mitochondria were more coupled, no changes in whole animal VO₂ were observed. Although our system detected the expected changes in VO₂ induced by fasting, no differences were observed between control and UCP3 KO mice in any of the states studied. These results indicate that either UCP3-uncoupling activity in muscle is not an important determinant of VO₂ in the whole animal or that other mechanisms are effectively compensating for the lack of UCP3. Normal fatty acid and glucose oxidation in isolated muscles together with the normal respiratory exchange ratio observed in whole animals suggest that UCP3 does not play a major role in fuel partitioning. But again, it cannot be com-

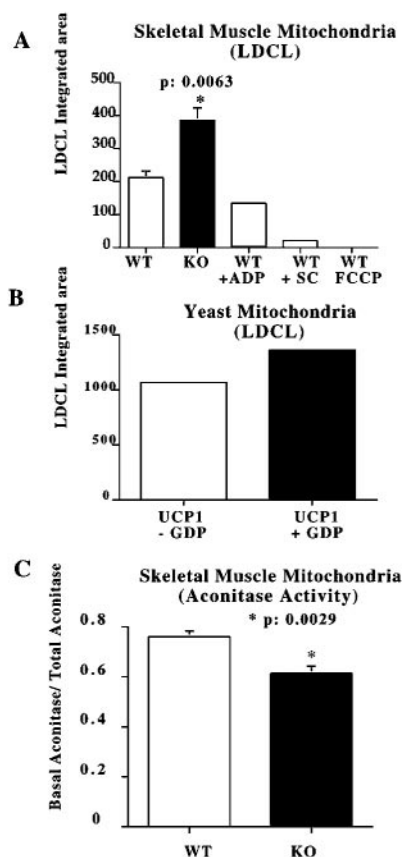


FIG. 5. **Oxidative stress.** A, LDCL in isolated skeletal muscle mitochondria. LDCL was monitored continuously for 10 min after incubation of mitochondria with $20 \mu\text{M}$ of lucigenin, as described under "Experimental Procedures." Data are expressed as the integrated area under the curve (46). The values represent the mean \pm S.E. of 4 mice, $p = 0.0063$; unpaired Student's t test. Shown is a representative experiment validating the LDCL assay. Skeletal muscle mitochondria from WT mice were incubated with 1 mM ADP, 0.5 mM SC52608 (SC), or $1 \mu\text{M}$ FCCP. Also shown is LDCL from skeletal muscle mitochondria isolated from UCP3 KO mice. B, LDCL in yeast mitochondria-expressing UCP1, incubated with and without 1 mM GDP. C, aconitase activity in isolated skeletal muscle mitochondria. Results are expressed as the ratio of basal aconitase activity to total aconitase activity (48), as described under "Experimental Procedures." The values represent the mean \pm S.E. of 6 mice, $p < 0.01$; unpaired Student's t test.

pletely excluded that UCP2 and/or UCP1 or another futile cycle could be compensating for the deficit of UCP3.

Several gene expression studies suggest that UCP3 could play an important role in exercise performance (25, 26). However, our data clearly show that the lack of UCP3 does not alter physical performance during acute exercise to exhaustion. The physical performance was also similar during the second round of exercise, indicating that KO and WT mice have similar recovery capacities post-exercise. Fatty acid and glucose oxidation after exercise did not reveal any impairment in exercise-induced alterations in skeletal muscle fuel utilization.

The role of UCP3 in cold exposure-induced thermogenesis was also studied. It is well established that UCP1 plays an important role in thermoregulation in rodents (50, 52, 53). Our data show that UCP3 KO mice exposed to cold have normal temperature homeostasis, indicating that unlike UCP1, UCP3 is not required for normal thermoregulation in response to cold exposure.

Several studies suggest that ROS production is a function of the mitochondrial membrane potential (34, 36, 54). It has been hypothesized that ROS are produced when the mitochondrial membrane potential is above a specific threshold. Indeed, ROS production is increased during state 4 respiration, when the

inner membrane mitochondrial potential is at its peak (33). An increase in mitochondrial membrane potential slows electron transport through the respiratory chain, resulting in an increase in the ubiquinone free-radical half-life (33). As a result, electrons have an increased probability of interacting with oxygen to form ROS. Thus, mild uncoupling of the mitochondria could be a mechanism to prevent the formation of oxygen free radicals (35). This mechanism could be important in skeletal muscle, given that it accounts for an important fraction of the total oxygen consumption at rest and that this fraction is even higher when skeletal muscle switches to maximal activity. On the other hand, superoxide anions are produced at high levels during the transition from anaerobiosis (*i.e.* anaerobic exercise) to reoxygenation (*i.e.* post-exercise) (55, 56).

To determine whether the production of ROS was increased in the UCP3 KO mouse skeletal muscle mitochondria, we used two independent approaches. The first was an *in vitro* method based on LDCL to detect superoxide anion production. Although there has been some concern about the specificity of the lucigenin assay (57), it has recently been shown that lucigenin can be used reliably with isolated mitochondria with concentrations up to $20 \mu\text{M}$ (46, 58). To validate this measurement, we studied LDCL in incubated mitochondria after the addition of a ROS scavenger, an uncoupler, and ADP, the latter two of which decrease the mitochondrial proton electrochemical gradient. As expected, each of these treatments decreased chemiluminescence. We also observed that LDCL was increased when UCP1-expressing yeast mitochondria were incubated with GDP, an inhibitor of UCP1-mediated uncoupling activity (52). We next used the LDCL method to assess ROS production in UCP3 KO skeletal muscle mitochondria. UCP3 KO skeletal muscle mitochondria have increased LDCL compared with wild type mitochondria. This finding suggests that skeletal muscle mitochondria lacking UCP3 produce more superoxide anions.

As a measure of oxygen free radical production *in vivo*, we assessed mitochondrial aconitase activity (57, 59) in skeletal muscle mitochondria. Aconitase enzymatic activity is inhibited by ROS and serves as an indicator of ROS production. Mitochondrial aconitase activity was decreased by 20–25% in UCP3 KO mice, indicating an increase in ROS production *in vivo*. As expected, no difference between WT and KO mice was observed in liver mitochondria (liver mitochondria do not express UCP3 protein), suggesting that the effect observed in skeletal muscle was specifically mediated by deficiency of UCP3. Thus, UCP3-mediated uncoupling may be physiologically important for minimizing production of ROS by skeletal muscle mitochondria. Increased ROS production in UCP3 KO mice could enhance oxidative damage to lipids, proteins, and DNA, accelerating the aging process (59). This possibility will be addressed in future studies.

In summary, we provide evidence that UCP3 KO mice are apparently healthy animals but have increased coupling of mitochondrial respiration in skeletal muscle mitochondria. This demonstrates that UCP3, expressed at endogenous levels, has uncoupling activity. Despite this, UCP3 does not seem to be required for body weight regulation, normal exercise tolerance, fatty acid oxidation, or cold-induced thermogenesis. The fact that genetic disruption of UCP3 does not affect these parameters despite altering mitochondrial coupling raises the possibility that compensatory mechanisms are occurring. We also show that mitochondria lacking UCP3 produce more ROS, suggesting that one of the functions of UCP3 could be to prevent excessive oxidative stress in skeletal muscle. The physiological relevance of this observation will be addressed in future studies.

Acknowledgments—We thank Dr. Tom Balon for advice on perform-

ing metabolite assays, Dr. Lawrence J. Sliker for providing UCP3 antibody, and Dr. Marc Reitman for communication of results (62).

REFERENCES

- Vidal-Puig, A., Solanes, G., Grujic, D., Flier, J. S., and Lowell, B. B. (1997) *Biochem. Biophys. Res. Commun.* **235**, 79–82
- Boss, O., Samec, S., Paoloni-Giacobino, A., Rossier, C., Dulloo, A., Seydoux, J., Muzzin, P., and Giacobino, J. P. (1997) *FEBS Lett.* **408**, 39–42
- Gong, D.-W., He, Y., Karas, M., and Reitman, M. (1997) *J. Biol. Chem.* **272**, 24129–24132
- Lin, C. S., and Klingenberg, M. (1980) *FEBS Lett.* **113**, 299–303
- Lin, C. S., Hackenberg, H., and Klingenberg, E. M. (1980) *FEBS Lett.* **113**, 304–306
- Fleury, C., Neverova, M., Collins, S., Raimbault, S., Champigny, O., Levi-Meyrueis, C., Bouillaud, F., Seldin, M. F., Surwit, R. S., Ricquier, D., and Warden, C. H. (1997) *Nat. Genet.* **15**, 269–272
- Gimeno, R. E., Dembski, M., Weng, X., Andrew, W., Shyjan, A. W., Gimeno, C. J., Iris, F., Ellis, S. J., Deng, N., Woolf, E. A., and Trataglia, L. A. (1997) *Diabetes* **46**, 900–906
- Sanchis, D., Fleury, C., Chomiki, N., Gubern, M., Huang, Q., Neverova, M., Gregoire, F., Easlick, J., Raimbault, S., Levi-Meyrueis, C., Miroux, B., Collins, S., Seldin, M., Richard, D., Warden, C., Bouillaud, F., and Ricquier, D. (1998) *J. Biol. Chem.* **273**, 34611–34615
- Mao, W., Yu, X. X., Zhong, A., Li, W., Brush, J., Sherwood, S. W., Adams, S. H., and Pan, G. (1999) *FEBS Lett.* **443**, 326–330
- Zhang, C. Y., Hagen, T., Mootha, V. K., Sliker, L. J., and Lowell, B. B. (1999) *FEBS Lett.* **449**, 129–134
- Jaburek, M., Varecha, M., Gimeno, R., Dembski, M., Jezek, P., Zhang, M., Burn, P., Trataglia, L. A., and Garlid, K. D. (1999) *J. Biol. Chem.* **274**, 26003–26007
- Klingenberg, M., Ehtay, K. S., Bienengraeber, M., Winkler, E., and Huang, S. G. (1999) *Int. J. Obes.* **23**, 24–29
- Klingenberg, M., and Huang, S. G. (1999) *Biochim. Biophys. Acta* **1415**, 271–296
- Jezek, P., Hanus, J., Semrad, C., and Garlid, K. D. (1996) *J. Biol. Chem.* **271**, 6199–6205
- Garlid, K. D., Orosz, D. E., Modriansky, M., Vassanelli, S., and Jezek, P. (1996) *J. Biol. Chem.* **271**, 2615–2620
- Garlid, K. D., Jaburek, M., and Jezek, P. (1998) *FEBS Lett.* **438**, 10–14
- Brand, M. D., Brindle, K. M., Buckingham, J. A., Harper, J. A., Rolfe, D. F. S., and Stuart, J. A. (1999) *Int. J. Obes.* **23**, (suppl.) 4–11
- Silva, J. E., and Rabelo, R. (1997) *Eur. J. Endocrinol.* **136**, 251–264
- Rolfe, D. F. S., and Brand, M. D. (1996) *Am. J. Physiol.* **271**, C1380–C1389
- Ravussin, E., Lilloja, S., Knowler, W. C., Christin, L., Freymond, D., Abbott, W. G., Boyce, V., Howard, B. V., and Bogardus, C. (1988) *N. Engl. J. Med.* **318**, 467–472
- Weigle, D. S., Selfridge, L. E., Schwartz, M. W., Seeley, R. J., Cummings, D. E., Havel, P. J., Kuijper, J. L., and Beltradelrio, H. (1998) *Diabetes* **47**, 298–272
- Hwang, C. S., and Lane, D. (1999) *Biochem. Biophys. Res. Commun.* **258**, 464–469
- Brun, S., Carmona, S. C., Mampel, T., Vinas, O., Giralt, M., Iglesias, R., and Villarroya, F. (1999) *FEBS Lett.* **453**, 205–209
- Gong, D.-W., He, Y., and Reitman, M. (1999) *Biochem. Biophys. Res. Commun.* **256**, 27–32
- Boss, O., Samec, C., Desplanches, D., Mayet, M. H., Seydoux, J., Muzzin, P., and Giacobino, J. P. (1998) *FASEB J.* **12**, 335–339
- Tsuboyama-Kasaoka, N., Tsunoda, N., Maruyama, K., Takahashi, M., Kim, H., Ikemoto, S., and Esaki, O. (1998) *Biochem. Biophys. Res. Commun.* **247**, 498–503
- Millet, L., Vidal, H., Andrealli, F., Larrouy, D., Riou, J. P., Risquier, D., Laville, M., and Langin, D. (1997) *J. Clin. Invest.* **100**, 26654–26670
- Leibel, R. L., Rosenbaum, M., and Hirsch, J. (1995) *N. Engl. J. Med.* **332**, 621–628
- Argyropoulos, G., Brown, A. M., Willi, S. M., Zhu, J., He, Y., Reitman, M., Gevaso, S. M., Spruill, L., and Garwey, W. T. (1998) *J. Clin. Invest.* **102**, 1345–1351
- Bouchard, C., Perusse, L., Chagnon, L., Warden, C., and Ricquier, D. (1997) *Hum. Mol. Genet.* **6**, 1887–1889
- Urhammer, S. A., Dalgaard, L. T., Sorensen, T. I., Tybjaerg-Hansen, A., Echwald, S. M., Andersen, T., Clausen, J. O., and Pedersen, O. (1998) *Diabetologia* **41**, 241–244
- Chung, W. K., Luke, A., Cooper, R. A., Rotini, C., Vidal-Puig, A., Rosenbaum, M., Chua, M., Solanes, G., Zheng, M., Zhao, L., LeDuc, C., Eisberg, A., Chu, F., Murphy, E., Scherer, M., Arrone, L., Caprio, S., Kahle, B., Gordon, D., Leal, S., Goldsmith, R., Andreu, A. L., Bruno, C., DiMauro, S., Heo, M., Lowe, J., Lowell, B. B., Allison, D. B., and Leibel, R. L. (1999) *Diabetes* **48**, 1890–1895
- Bodrova, M. E., Dedukhova, V. I., Mokhova, E. N., and Skulachev, V. P. (1998) *FEBS Lett.* **435**, 269–274
- Skulachev, V. P. (1997) *Biosci. Rep.* **17**, 347–364
- Papa, S., and Skulachev, V. P. (1997) *Mol. Cell. Biochem.* **174**, 305–309
- Skulachev, V. P. (1998) *Biochim. Biophys. Acta* **1363**, 100–124
- Boveris, A., and Chance, B. (1973) *Biochem. J.* **134**, 707–716
- Susulic, V. S., Frederic, R. C., Lawitts, J., Tozzo, E., Kahn, B. B., Harper, M. E., Himms-Hagen, J., Flier, J. S., and Lowell, B. B. (1995) *J. Biol. Chem.* **270**, 29483–29492
- Li, E., Suvov, H. M., Lee, K. F., Evans, R. M., and Jaenisch, R. (1993) *Proc. Natl. Acad. Sci. U. S. A.* **90**, 1590–1594
- Boss, O., Bachman, E., Vidal-Puig, A., Zhang, C. Y., Peroni, O., and Lowell, B. B. (1999) *Biochem. Biophys. Res. Commun.* **261**, 870–876
- Vidal-Puig, A., Jimenez-Linan, M., Lowell, B. B., Hamann, A., Hu, E., Spiegelman, B., Flier, J. S., and Moller, D. E. (1996) *J. Clin. Invest.* **97**, 2553–2561
- Jaworek, D., Gruber, W., and Bergmeyer, H. U. (1974) in *Methods of Enzymatic Analysis* (Bergmeyer, H. U., ed) Vol. 4, pp. 2127–2131, Verlag-Chemie, Weinheim/Academic Press, New York
- Deleted in proof
- Salmon, D. M., and Flat, J. P. (1985) *Int. J. Obes.* **9**, 443–449
- Muioio, D. M., Dohm, G. L., Fiedorek, F. T. J., Tapscott, E. B., and Coleman, R. A. (1997) *Diabetes* **46**, 1360–1363
- Li, Y., Zhu, H., Kuppusamy, P., Roubaud, V., Zweier, J. L., and Trush, M. A. (1998) *J. Biol. Chem.* **273**, 2015–2023
- Kasten, T. P., Settle, S. L., Misko, T. P., Riley, D. P., Weiss, R. H., Currie, M. G., and Nickols, G. A. (1995) *Proc. Soc. Exp. Biol. Med.* **208**, 170–177
- Hausladen, A., and Fridovich, I. (1996) *Methods Enzymol.* **269**, 37–41
- Himms-Hagen, J. (1989) *Prog. Lipid Res.* **28**, 67–115
- Enerback, S., Jacobsson, A., Simpson, E. M., Guerra, C., Yamashita, H., Harper, M. E., and Kozak, L. P. (1997) *Nature* **387**, 90–94
- Boss, O., Bobbioni-Harsh, E., Assimacopoulos-Jeannet, F., Muzzin, P., Munger, R., and Giacobino, G. P. (1998) *Lancet* **351**, 1933
- Nicholls, D. G., and Locke, R. M. (1984) *Physiol. Rev.* **64**, 1–64
- Nicholls, D. G., and Rial, E. (1984) *Trends Biochem. Sci.* **1984**, 489–491
- Negre-Salvayre, A., Hirtz, C., Carrera, G., Cazenave, R., Trolly, M., Salvayre, R., Penicaud, L., and Castiella, L. (1997) *FASEB J.* **11**, 809–815
- Du, G., Mouithys-Mickalad, A., and Sluse, F. E. (1998) *Free Radic. Biol. Med.* **25**, 1066–1074
- Bejma, J., and Ji, L. L. (1999) *J. Appl. Physiol.* **87**, 465–470
- Fridovich, I. (1997) *J. Biol. Chem.* **272**, 18515–18517
- Li, Y., Zhu, H., and Trush, M. A. (1999) *Biochim. Biophys. Acta* **28**, 1–12
- Gradner, P. R., Rainieri, I., Epstein, L. B., and White, C. W. (1995) *J. Biol. Chem.* **270**, 13399–13405
- Deleted in proof
- Adra, C. N., Boer, P., and McBurney, M. W. (1987) *Gene* **60**, 65–74
- Gong, D.-W., Monemdjou, S., Gavrilova, O., Leon, L. R., Marcus-Samuels, B., Chou, C. J., Everett, C., Kozak, L. P., Li, C., Deng, C., Harper, M. E., and Reitman, M. L. (2000) *J. Biol. Chem.* **275**, 16251–16257